Proceedings of ASME Turbo Expo 2011
GT2011
June 6-10, 2011, Vancouver, British Columbia, Canada

GT2011-46635

INVESTIGATION OF TRANSIENT CFD METHODS APPLIED TO A TRANSONIC COMPRESSOR STAGE

Rob Blumenthal
ANSYS, Inc.
El Dorado Hills, CA, USA

Brad Hutchinson
ANSYS Canada, Ltd.
Waterloo, ON, Canada

Laith Zori,
ANSYS Inc
Lebanon, NH, USA

ABSTRACT

Understanding unsteady flow phenomena in compressor stages often requires the use of time-accurate CFD simulations. Due to the inherent differences in blade pitch between adjacent blade rows, the flow conditions at any given instant in adjacent blade rows differ. Simplified computation of the stage represented by a single blade in each row and simple periodic boundary conditions is therefore not possible. Depending on the blade counts, it may be necessary to model the entire annulus of the stage; however, this requires considerable computational time and memory resources.

Several methods for modeling the transient flow in turbomachinery stages which require a minimal number of blade passages per row, and therefore reduced computational demands, have been presented in the literature. Recently, some of these methods have become available in commercial CFD solvers. This paper provides a brief description of the methods used, and how they are applied to a transonic compressor stage. The methods are evaluated and compared in terms of computational efficiency and storage requirements, and comparison is made to steady stage simulations. Comparisons to overall performance data and two-dimensional LDV measurements are used to assess the predictive capabilities of the methods. Computed flow features are examined, and compared with reported measurements.

INTRODUCTION

End users of gas turbines, whether used on land, sea or in the air, demand on-going improvements to their machines. “Improved” is context dependent, and may mean improved efficiency, reduced emissions, reduced noise or increased reliability and durability. The compressor, being a key engine component, is required to operate efficiently over the widest possible range, with high stage loadings. Designers are challenged to meet ever-escalating targets in a competitive, time-critical environment. While experience and testing are essential to the process, advanced simulation tools are key enablers.

One-dimensional, throughflow and in recent years, steady multistage CFD solvers are key aerodynamic analysis tools in the designer’s toolbox. The latter is a powerful tool, able to simulate several blade rows, including secondary/leakage flows and over-tip flows, in addition to the primary flow. A limitation is that while meridional information is effectively transferred from one component to the next, blade-to-blade information is effectively only available on a local basis, and is lost across the component interface as a result of the circumferential averaging process. The real flow in a compressor is clearly transient in nature, although in many circumstances a steady approximation seems to be effective. However, as stage loadings increase, as operation approaches stall and the requirement for predictive precision increases the suitability of the steady approximation may decrease. For these reasons designers and analysts wish to consider fully transient methods.

This paper compares both steady and transient CFD methods, to each other, and against experimental data, with the goal of assessing their efficiency, accuracy and utility in helping the designer/analyst evaluate and understand unsteady compressor flows.

NOMENCLATURE

BPF	Blade Passing Frequency
FT	Fourier Transformation
LE	Leading edge
PT	Profile Transformation
SST	Shear Stress Transport turbulence model
TRS	Transient Rotor-Stator
TE	Trailing edge
TT	Time Transformation

1.0 SOLUTION METHODS

Four transient solution methods were used to simulate the flow in a transonic axial compressor stage. A brief description of these methods is provided below. In addition, steady state solutions were obtained, and besides the experimental data, they provide a basis against which to compare the transient calculations.

Simulations were performed using a pre-release version of ANSYS CFX R13.0. All solutions were obtained using second-order spatial and temporal discretization. The fluid was modeled as an ideal gas with constant properties, and results are provided with two turbulence treatments. One set of calculations assumed the flow as fully turbulent, using the SST turbulence model [Menter, 1994]. The second considered the flow as transitional, and augmented the SST model with the Γ-Θ transition model [Menter et al., 2004].

The Transient Rotor-Stator (TRS) implementation uses a fully implicit and conservative discretization at the interface where the rotor meets the stator and accounts for the circumferential position of the rotor relative to the stator. The method is usually used to model a full wheel or in some situations a sector of the wheel where standard periodicity can be imposed with no approximation. The current TRS implementation also allows for modeling a single blade passage per row, even though the pitch lengths of the adjacent rows differ, by imposing standard periodicity on pitchwise boundaries and automatically stretching or compressing the flow profile across the rotor-stator interface [Galpin et al., 1995, and ANSYS, 2009]. This variant of the TRS implementation is referred to as the Profile Transformation (PT) method. It provides a fast and robust approximate transient solution without the need for geometrically scaling or modifying the blade geometry. To reduce the pitch-scaling error multiple passages can be used so that the ensemble pitch ratio is closer to unity. For example, for the case of a rotor with 36 blades and a stator with 46 blades, the pitch ratio is 1.278 if only a single passage of each component is modeled. However, if two rotors and three stators are modeled the ratio is 0.852, and three rotors with four stators yields 0.958. While some error is involved with a non-unity pitch ratio, the computational cost is much less than modeling the 18 rotor and 23 stator passages required to achieve unity pitch ratio.

An improvement to the Profile Transformation method is the recently developed Time Transformation (TT) method [Biesinger et al., 2010], which is an evolution of the time-inclining method [Giles, 1988]. The flow equations are transformed in time to ensure that the pitchwise boundaries are truly periodic. The implicit nature of the formulation maintains solution robustness and also accounts for the correct blade passing signals between the rotor and stator. A limitation on this method is that the transformation in time puts a physical constraint on the range of possible stage pitch ratios, beyond which numerical instabilities will be encountered [Giles, 1988]. However, in practice this is not a serious limitation in that it can easily be overcome by adjusting the number of passages solved, as described for the PT method, so that the ensemble pitch ratio is closer to unity.

The fourth transient method is the Fourier Transformation (FT) method. In this method the flow history on the phase-shifted pitchwise boundaries are stored using Fourier series at the blade passing frequency and its higher harmonics [He, 1990]. To improve the quality of the signal representation and to speed convergence to a transient periodic solution this implementation uses a double-passage technique. The Fourier coefficients of a flow variable are therefore collected at the interface between the two passages and then applied on both sides of the pitchwise periodic boundaries ("upper" and "lower" circumferential boundaries of the two-passage ensemble), with appropriate phase-shift, to reconstruct the appropriate boundary values [Biesinger et al., 2010]. On the interface between the rotor and the stator, flow information is stored using double-Fourier series by decomposing the solution history in time and azimuthal direction [Gerolymos et al., 2002]. The solution is then reconstructed on each side of the interface using Fourier coefficients from the opposite side. This strategy provides excellent data compression by taking advantage of the periodic nature of the flow in azimuthal direction. An attractive feature of this method is that it is applicable to all rotor speeds and to large pitch ratios, for example such as that encountered when modeling the fan inlet distortion problem.

Besides transient solutions, steady state "stage" [Galpin et al., 1995] solutions were also obtained. These steady solutions provided a starting point for the transient solutions, and are also interesting to compare to the transient solutions from the point of view of computational cost and solution results.

2.0 AXIAL COMPRESSOR STAGE MODEL

The subject of the study was the NASA transonic compressor stage consisting of NASA Rotor 35 with

NASA Stator 37, as described by Van Zante [1998] and Van Zante et al. [2002]. The rotor consisted of 36 blades, and the stator 46 blades. Table 1 summarizes the pertinent details of the stage as well as simulation information. Figure 1 provides a meridional view of the computational domain and also displays the medium mesh on the surface of the blades. The computational domain was constructed such that the inlet was approximately 1.5 axial rotor chord lengths upstream of the rotor leading edge, and the exit approximately 2.0

Table 1 NASA Stage simulation information

# of rotor blades	36
# of stator blades	46
Rotational speed	13,750 RPM
Rotor axial chord (hub)	41.18 mm
Stator axial chord (hub)	35.71 mm
Rotor tip clearance	0.61 mm
Stator tip clearance	0.51 mm
Inlet total pressure	101.2 kPa
Inlet total temperature	288.1 K
Inlet turbulence intensity	5%
Flow rate (% of design)	100%
Flow rate	17.19 kg/s
Domain inlet axial location	-61.0 mm
Inlet axial measurement location	-42.4 mm
Rotor LE axial location (hub)	0.00 mm
Stator TE axial location (hub)	82.1 mm
Exit axial measurement location	106.7 mm
Domain exit axial location	152.4 mm

stator chord lengths downstream of the stator trailing edge. Upstream and downstream experimental measurement locations are well within the computational domain, as indicated in Figure 1.

Three computational grids were generated using the ANSYS TurboGrid software, and details are provided in Table 2. The grids (approximately) successively double in size by increasing the blade-to-blade and streamwise node count. In each case the near wall region of the flow is resolved by an O-grid with 16 nodes, with near wall

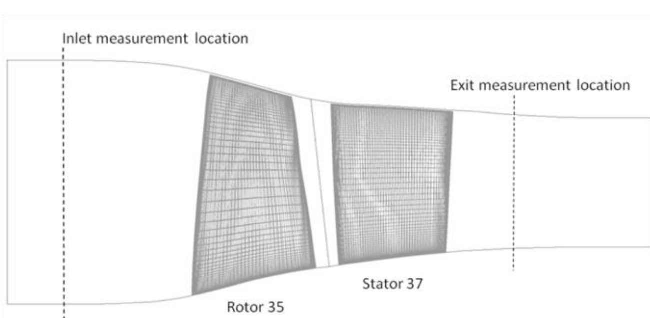

Figure 1: Geometry, mesh on blades and computational domain for the stage

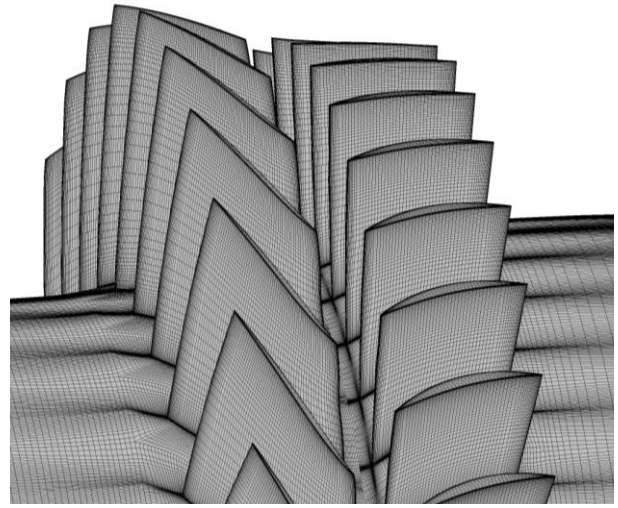

Figure 2: Medium grid on rotor (left) and stator (right) and on hub.

spacing yielding a Y-plus of approximately 1.2. All grids resolved the blade tip region with 16 nodes from tip to shroud. The total number of nodes is divided roughly equally between the rotor and the stator. Figure 2 provides a three-dimensional view of the grid on the blades and hub. Figure 3 shows the mesh at the rotor leading edge, hub, and stator trailing edge, hub.

The inlet boundary conditions for the CFD simulations were specified constant total pressure, total temperature and turbulence intensity. Mass flow was prescribed at the outlet. The grid information provided in Table 2 is for one rotor and one stator passage. The number of passages simulated and hence the actual grid size depends on the method used. The stage and TT simulations used one rotor and one stator passage, so the grid sizes are as listed in Table 2. The FT method solves for two rotor and stator passages, so the actual number of nodes solved is almost double that listed. The reference solution solved for one half the domain: 18 rotors and 23 stators, with a total grid size of 29.9 million nodes (medium grid). Three PT solutions were obtained. One solved for one rotor and one stator, for which the pitch ratio is 1.278, the second for two rotors and three stators with ensemble pitch ratio of 0.852 and the third for three rotors and four stators, with ensemble pitch ratio of 0.958. The FT and TT methods were solved using 115 time steps per rotor sweep, which was probably more than necessary given the spatial grid resolution. The PT and TRS methods used 60 time steps per rotor pass.

Table 2 NASA stage grid information (one stator and one rotor passage)

Grid size	Total Nodes (stator + rotor)	Nodes in span (rotor/stator)	Averag e Blade Y+
Coarse	739,000	91/98	1.2
Medium	1,475,000	96/106	1.2
Fine	3,235,000	96/106	1.2

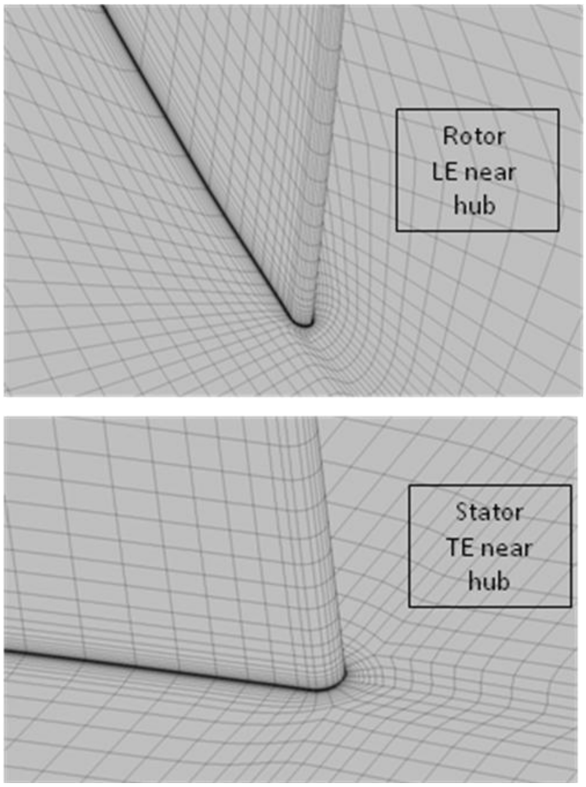

Figure 3: Medium grid on hub at rotor LE (upper) and stator TE (lower).

3.0 COMPUTATIONAL RESULTS

The solutions obtained and overall aerodynamic predictions are summarized in Table 3. The steady and time-averaged predictions of total pressure ratio, total temperature ratio and adiabatic efficiency are relative to the inlet and exit measurement planes indicated in Figure 1. The left column indicates the method, the grid size and the turbulence model used for the particular simulation:

- Method: “ST” = stage (steady simulation), “PT” = Profile Transformation, “TT” = Time Transformation, “FT” = Fourier Transformation, “½ TRS” = half domain, Transient Rotor Stator, reference solution
- Grid: “C” = coarse, “M” = medium, “F” = fine.
- Turbulence: “T” = SST turbulence model, no transition, “LT” = SST turbulence model with laminar-turbulent transition.

Also included in the table are results reported by Van Zante et al. [2002]. “Van Zante -A” refers to their results obtained with the APNASA CFD code, “Van Zante -M” to their results with the MSU-Turbo CFD code, and “Expt.” indicates measured experimental data.

Table 3 NASA stage steady and unsteady simulation results

Method-Grid-Turbulence	Total Pressure Ratio	Total Temper-ature Ratio	Efficiency (isentropic)
ST-C-T	1.419	1.123	85.9
ST-M-T	1.434	1.125	86.9
ST-F-T	1.451	1.128	87.6
ST-C-LT	1.435	1.125	87.3
ST-M-LT	1.449	1.127	88.2
ST-F-LT	1.464	1.129	88.9
TT-M-T	1.431	1.125	86.4
PT-M-LT (1-1)	1.447	1.127	87.9
PT-M-LT (2-3)	1.445	1.126	88.1
PT-M-LT (3-4)	1.445	1.126	88.0
TT-M-LT	1.445	1.126	87.8
FT-M-LT	1.449	1.128	87.2
½ TRS-M-LT	1.446	1.126	88.6
Van Zante -A	1.44	1.126	87.6
Van Zante -M	1.46	1.130	87.1
Expt.	1.40	1.113	88.5

3.1 Steady simulations

Overall steady state (“stage”) performance predictions are provided in Table 3 and Figures 4 and 5, along with the transient predictions. The grid refinement studies show that predictions of total pressure, total temperature and adiabatic efficiency all increase with grid size, although the rate of change decreases with increase in grid size. Nevertheless, for reasons of computational economy, the medium grid was selected for the transient simulations.

The table and figures also indicate a substantial difference between the fully turbulent predictions and those that include the effects of laminar-turbulent transition. The adiabatic efficiency is about 1.2 to 1.3 percentage points higher for the transition case. It seems that the majority of this difference comes from the rotor, since adiabatic efficiency predicted over the rotor alone shows a difference of about 0.9 percentage points. Figure 6 displays the wall shear and streaklines on the suction side of Rotor 35 for the fully turbulent (left) and transitional (right) simulations. The fully turbulent case indicates high shear stresses at the leading edge, increasing with radius. For the upper half of the blade, following a streakline from the leading edge, the shear stress drops abruptly, coinciding with the shock and a small region of localized separation. The shear stress then redevelops with streamwise distance as the boundary layer grows. For the transitional case, the leading edge region shear stresses are much lower, due

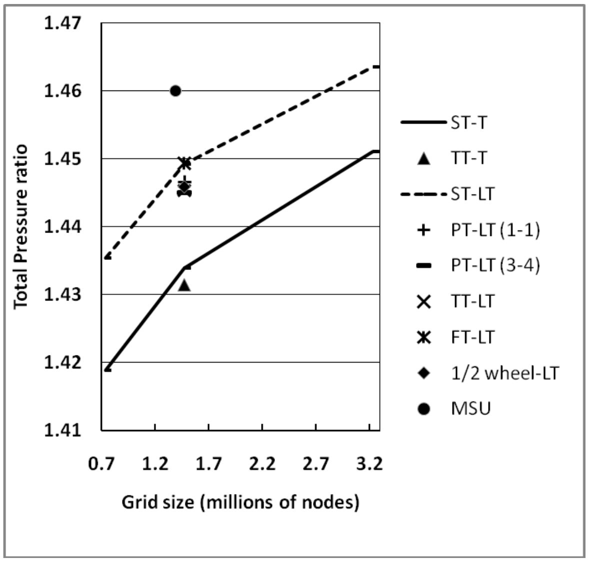

Figure 4: Predicted stage performance: total pressure ratio

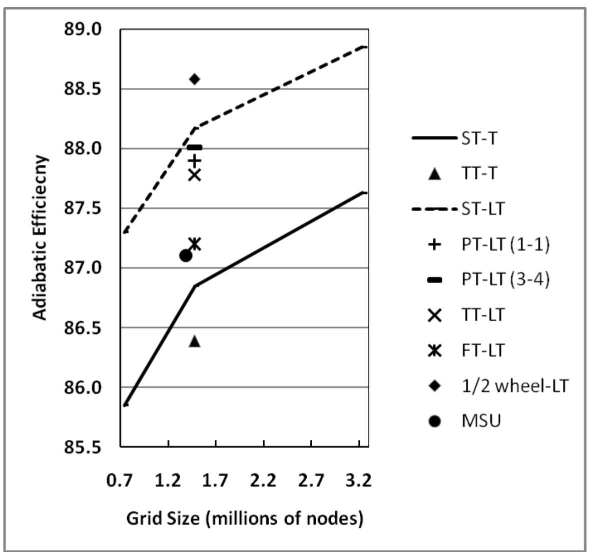

Figure 5: Predicted stage performance: adiabatic efficiency

to the laminar boundary layer. The predicted separated flow region is a little larger before reattachment and subsequent boundary layer development.

3.2 Transient simulations

Transient simulations were performed on the medium grid only, and the overall performance predictions are provided in Table 3 and Figures 4 and 5, along with the steady results. The transient and steady predictions are in reasonable agreement, with the transient results generally slightly smaller in magnitude. The predicted

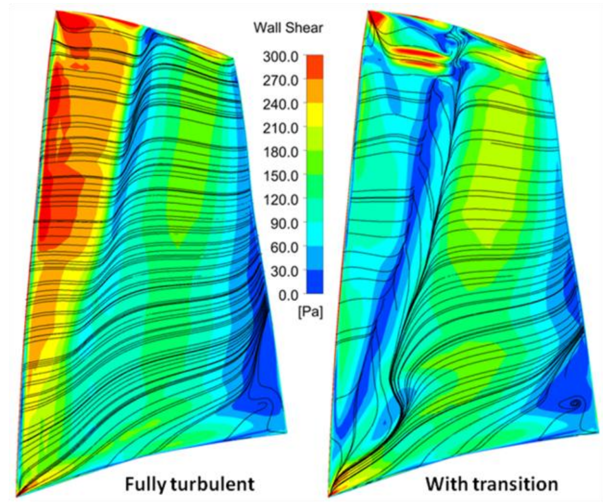

Figure 6: Rotor 35, suction side wall shear stress and streaklines. Medium grid, steady. Fully turbulent (left), with transition (right)

difference between fully turbulent and laminar-turbulent adiabatic efficiency is the same as for the steady simulation (1.3%, TT method).

Also reported in Table 3 are experimental results and numerical predictions reported by Van Zante et al. Their “MSU-Turbo” predictions are included in Figures 4 and 5. The present predictions are in reasonable agreement with the former. What is somewhat surprising is the following: all predictions of total pressure and total temperature are significantly above experiment. Nevertheless, predictions of efficiency are in reasonable agreement with the experimentally derived value of 88.5%. Over prediction of total temperature and pressure do not seem to be a numerical issue: both grid refinement and improved modeling fidelity (including laminar-turbulent transition, for instance) point to higher values still. For the present calculations, the only effect that serves to reduce predicted values is transient simulation, instead of steady. While the reduction is not sufficient to match the data, the predicted efficiency drops below experimental, for all but one case. The source of the discrepancy can only be speculated on. It might relate to use of incorrect geometry or clearances in the simulations, use of a mass flow boundary condition that is slightly too low, inlet boundary layer or an as yet unidentified numerical modeling shortcoming that afflicts all of the solvers used to predict this flow. The authors have insufficient knowledge of the experimental rig to speculate on possible experimental error.

As discussed previously, the TT method can be considered a correction to the more approximate PT method, and the predictions confirm this. Table 3 and Figures 4 and 5 indicate that the predictions from the two methods are quite close, even for the 1-rotor 1-stator case where the profile stretching is considerable, with a pitch

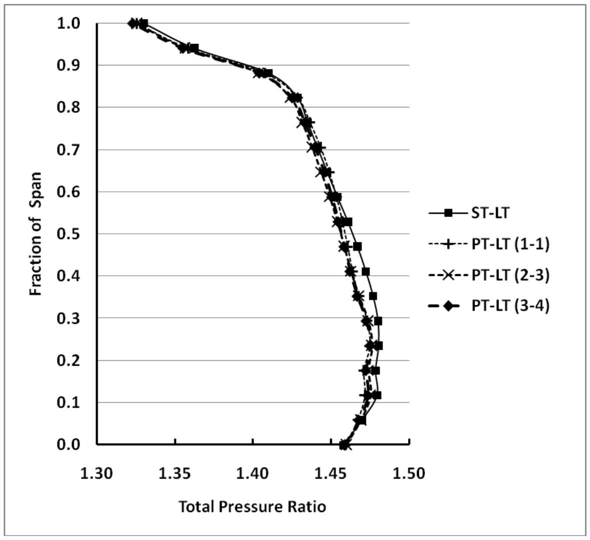

Figure 7: Circumferentially averaged stage total pressure ratio, at outlet measurement plane

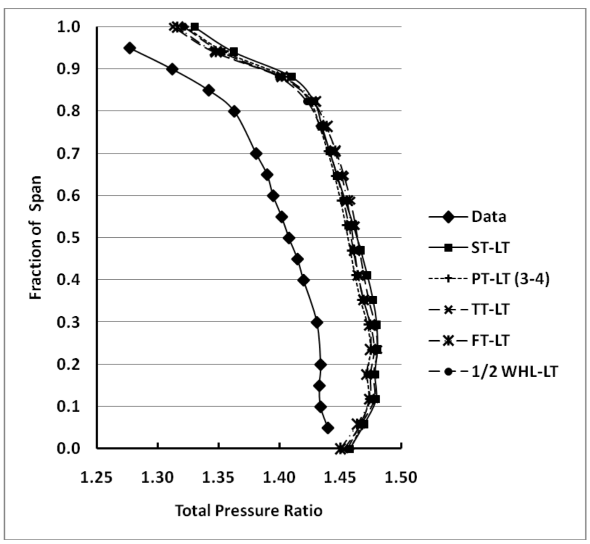

Figure 8: Circumferentially averaged stage total pressure ratio, at outlet measurement plane

ratio of 1.278. The predictions of total pressure and total temperature seem to approach those of the TT case as the ensemble pitch average approaches 1.0.

Circumferential averages of total pressure and total temperature, for the exit measurement plane, are presented in Figures 7 through 10. Figures 7 and 9 display results for the three PT calculations and the stage calculations. The total pressure profile is nearly identical for all three PT methods, and quite close to the steady

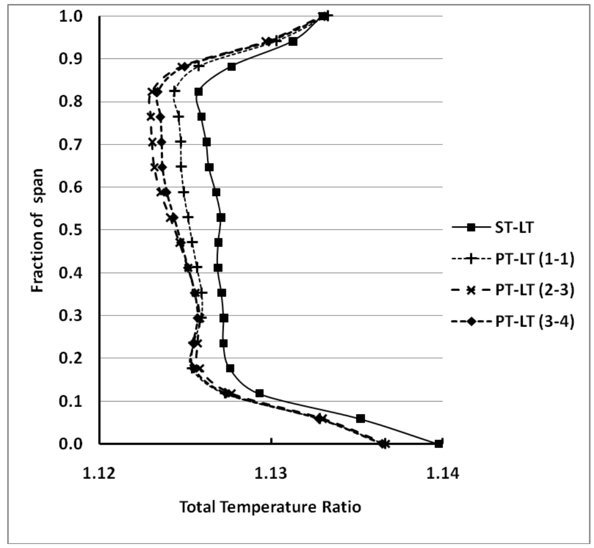

Figure 9: Circumferentially averaged stage total temperature ratio, at outlet measurement plane

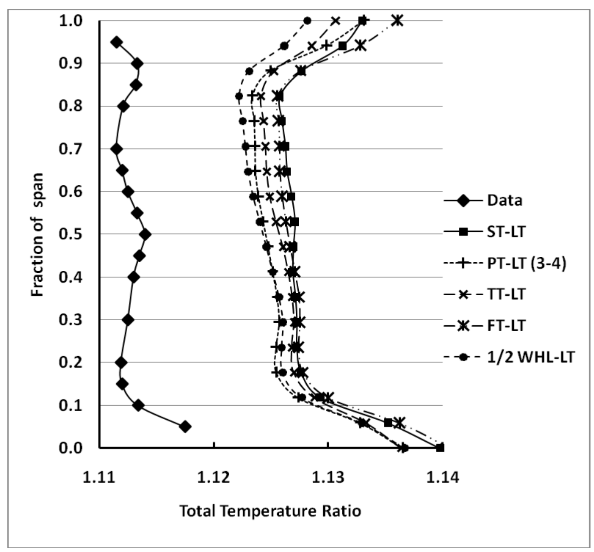

Figure 10: Circumferentially averaged stage total temperature ratio, at outlet measurement plane

predictions, while slightly greater variation is seen for total temperature. The 2-to-3 case (ensemble pitch ratio 0.852) is very close to the 3-to-4 case (ensemble pitch ratio 0.958). Figures 8 and 10 indicate that the data are lower than the predictions, as is the case for the overall performance predictions. The shape of the predicted total pressure profile is similar to the data, and all predictions are quite similar, departing little from the steady predictions. The total temperature predictions show greater variation. The PT and TT predictions are the closest in value, as anticipated, and in close agreement with the reference (1/2 wheel) solution. Results are slightly lower than the steady prediction, while the FT prediction at the shroud is greater than the steady prediction, indicating a slightly different flow pattern.

Relative computational effort is summarized in Table 4 for the various simulations. Column 2 lists the number of rotor passes required to achieve a repeating solution. The third column lists the number of non-linear coefficient updates per time step. The steady value is the number of iterations to convergence (200) divided by the number of time steps for the transient cases (60), yielding an equivalent effort. The fourth column lists the equivalent grid size, which takes the total number of passages in a given simulation and divides by 2. The fifth column is the product of columns 2 through 4, normalized by the steady result.

Table 4 indicates that the transformation method solutions require roughly an order of magnitude more computing than a steady solution, but are also an order of magnitude less expensive than the half-annulus reference case. The grid size is also an order of magnitude smaller, hence the hardware cost is much lower given that solutions can be obtained on roughly an order of magnitude fewer processors, for equivalent turnaround time.

Table 4 R35/S37 stage computational effort

Method-Grid	# of Rotor Passes	# of Coeff. Updates	Relative Grid Size	Relativ e Effort
ST-M	1	3.4	1	1.0
PT-M 1/1	6	4	1	7.1
PT-M 2/3	10	5	2.5	36.8
PT-M 3/4	6	5	3.5	30.9
TT-M	15	5	1	22.1
FT-M	6	4	2	14.1
½ -M	10	5	20.3	298.5

CONCLUSIONS

Steady and transient CFD simulations of the NASA Rotor 35/Stator 37 stage were performed and compared with each other, with measurement data and with earlier predictions. Simulations were performed at the design flow rate only, and so conclusions given here may differ than what might be observed at different flow points.

1. Computed stage overall total pressure and total temperature, both steady and transient, were above reported measurements. Van Zante et al. reported a similar result, and to that extent those and the current predictions are in qualitative agreement.
2. Improving the numerical prediction by refining the grid and including the effect of laminar-turbulent transition actually drives the predictions further from the measured data. This suggests some difference between the experiment and the simulation. One can only speculate at the cause: it could be one or more of a) mis-matched flow point, b) inlet boundary profiles significant and not accounted for, c) running a slightly different speed than reported, d) geometry differs from that used, e) tip clearance used in the simulation does not match experiment, f) neglect of leakage flows g) some unknown deficiency in physics that afflicts the present software and also that used by Van Zante et al.
3. The transient predictions of total pressure and total temperature are in slightly better agreement with the data, but the improvement in agreement is small relative to the spread.
4. The difference in fully turbulent and laminar-turbulent predictions is significant. The magnitude of the "delta" is the same for steady and transient predictions.
5. Predictions of stage overall adiabatic efficiency are for most cases slightly low compared to data but in reasonable agreement with the results of Van Zante et al.
6. There are small differences in the predictions of the various transformation methods. This may be expected since each makes slightly different approximations. Therefore, the practitioner would be advised to select one method or one combination of methods and use that consistently, and not switch among the various methods in order to obtain consistent predictions.
7. The PT and TT methods are in close agreement with each other and with the reference (half annulus) solution. In this work we are considering performance and not vibration, where it is known that the PT method will be slightly in error due to pitch scaling. With this limitation in mind, the PT method is attractive since its use is not restricted to a single stage.
8. While the transformation methods are an order of magnitude more expensive than steady simulations, if unsteady simulations are desired, for this case they are very attractive in that computational effort and resources are an order of magnitude less expensive than solving the full annulus (or half-annulus, in this case).
9. In this work, predictions were obtained at design flow point only, and hence represent a preliminary investigation of the methods. Future work will investigate the methods across the flow map. While it is presumed that the transient methods will be of

considerable utility off-design (particularly at low flow), that remains to be demonstrated. In addition, details of the flow will be examined to better understand the small differences between the various methods (for instance the small discrepancy in near-shroud total temperature between the FT and the other methods, as observed in Figure 10). One possible explanation which requires further investigation is the method of averaging and post-processing the predicted data in time and space. It is not clear that this is consistent for all methods and hence requires further examination in future work.

10. The current study dealt with two components (a single stage) only. The TT method is limited to a single stage; however, the PT and FT methods have no such limitation and theoretically could be used for multi-stage predictions.

ACKNOWLEDGMENTS

The authors wish to acknowledge Dr. Dale Van Zante of the NASA Glenn Research Center for providing information on the NASA Rotor 35 – Stator 37 compressor stage and Dr. Rubens Campregher, Dr. Philippe Godin, Mr. Robin Steed and Mr. Ryan O'Connor of ANSYS, Inc. for their assistance with the simulations and post-processing.

REFERENCES

ANSYS CFX Version 12 documentation, ANSYS Inc., 2009

Biesinger T., Cornelius C., Rube C., Schmid G., Braune A., Campregher C., Godin P., Zori L, 2010, "Unsteady CFD Methods in a Commercial Solver For Turbomachinery Applications", Proceedings of the ASME Turbo Expo 2010, GT2010-22762

Galpin P.F., Broberg R.B., Hutchinson B.R., "Three-Dimensional Navier Stokes Predictions of Steady State Rotor/Stator Interaction with Pitch Change", Third Annual Conference of the CFD Society of Canada, June 25-27, 1995, Banff, Alberta, Canada

Gerolymos G., Michon G., Neubauer J., 2002, "Analysis and Application of Chorochronic Periodicity in Turbomachinery Rotor/Stator Interaction Computations", Journal of Propulsion and Power, Vol 9, no. 6, pp. 1139-1152

Giles, M., 1988, "Calculation of Unsteady Wake/Rotor Interaction", Journal of Propulsion and Power, 4(4), pp. 356–362

He, L., 1990, "An Euler Solution for Unsteady Flows around Oscillating Blades", ASME Journal of Turbomachinery, 12, pp. 714–722

Menter, F.R., 1994, "Two-equation eddy-viscosity turbulence models for engineering applications", AIAA-Journal, 32, (8), pp. 1598 – 1605

Menter, F.R., Langtry, R.B., Likki, S.R., Suzen, Y.B., Huang, P.G., 2004, "A Correlation Based Turbulence Model Using Local Variables, Part 1 – Model Formulation", Proceedings of the ASME Turbo Expo 2004, GT2004-53452

Van Zante, D.E., "Study of a Wake Recovery Mechanism in a High-Speed Axial Compressor Stage", NASA/CR-1998-206594, February 1998.

Van Zante, D.E., To, W.M., Chen, J.P., "Blade Row Interaction Effects on the Performance of a Moderately Loaded NASA Transonic Compressor Stage", Proceedings of the ASME Turbo Expo 2002, GT2002-30575

